

# On the Red Shift of Hydrogen Like Spectral Lines in Plasmas

P. SANDERS<sup>1</sup> AND E. OKS<sup>1</sup>

<sup>1</sup>Physics. Department, 206 Allison Lab., Auburn University, Auburn, AL 36849, USA

**ABSTRACT:** Red shifts of spectral lines (hereafter, SL) play an important role in astrophysics. For inferring the relativistic red shifts from the observed red shifts it is required to allow for the Stark shift of SL. In laboratory plasmas, measurements of the Stark shift can supplement measurements of the Stark width and thus enhance plasma diagnostics – specifically the determination of the electron density. In the present paper we describe a new source of the Stark shift of hydrogenlike SL. It originates from configurations where the nearest perturbing ion is within the radiating atom/ion (“penetrating configurations”). As an example, we compare the results with the experimental shift of the Balmer-alpha SL of He II 1640 Å measured in a laboratory plasma by Pittman and Fleurier (Phys. Rev. A 33 (1986) 1291). We show that the allowance for this new additional red shift leads to a good agreement with the measured shift for the entire range of the electron density employed in that experiment, while without this new shift the previously known shifts underestimated the measured shift by factors between two and five.

## 1. INTRODUCTION

Red shifts of spectral lines (hereafter, SL) play an important role in astrophysics. Indeed, the relativistic (cosmological and gravitational) red shifts (see, *e.g.* book [1]) are at the core of models of the Universe and of tests for the general relativity. However, for inferring the relativistic red shifts from the observed red shifts it is required to allow for the Stark shift of SL. Hydrogen and hydrogenlike (hereafter, H-like) SL in plasmas are usually shifted to the red by electric microfields – see, *e.g.*, books [2, 3] and references therein. Besides, in laboratory plasmas, measurements of the Stark shift can supplement measurements of the Stark width and thus enhance plasma diagnostics – specifically the determination of the electron density (see, *e.g.*, paper [4]).

In the present paper we describe a new source of the Stark shift of H-like SL—in addition to the previously known sources of the shift (we call the latter “standard shifts”). As an example, we compare the results with the experimental shift of the Balmer-alpha SL of He II 1640 Å measured in a laboratory plasma by Pittman and Fleurier [5]. We show that the allowance for this new additional red shift leads to a good agreement with the measured shift from [5] for the entire range of the electron density employed in that experiment, while without this new shift the standard shifts underestimated the measured shift by factors between two and five.

## 2. “STANDARD” SHIFTS OF HYDROGENLIKE SPECTRAL LINES

One of the most significant “standard” contributions to the shift of H-like SL is caused by quenching (non-zero  $\Delta n$ ) [6] and elastic (zero  $\Delta n$ ) [7] collisions with plasma electrons—hereafter, the electronic shift (see also paper [8]).

There is also a so-called plasma polarization shift (PPS), which plays an important role in explaining the observed shifts of the high- $n$  H-like SL—see, *e.g.*, books [2, 9] and paper [10]. The PPS is less significant for the low- $n$  H-like SL. Physically the PPS is caused by the redistribution of plasma electrons due to the attraction to the radiating ion. When only plasma electrons inside the orbit of the bound electron were taken into account, the

resulting theoretical PPS was blue (such as, *e.g.*, in paper [11]). Later it was found that after the allowance for redistributed plasma electrons both outside and inside the bound electron orbit, the resulting theoretical PPS becomes red. However, theoretical results for red PPS by different authors differ by a factor of two – more details and the references will be provided below while comparing theoretical and experimental results.

Then there is a controversial issue of the ‘standard’ shift caused by plasma ions—hereafter, the standard ionic shift. Various existing calculations were based on the multipole expansion with respect to the ratio  $r_{\text{rms}}/R$  (in the binary description of the ion microfield) or with respect to the analogous parameter  $r_{\text{rms}} F^{1/2}$  (in the multi-particle description of the ion microfield  $F$ ). Here  $r_{\text{rms}}$  is the root-mean-square value of the radius-vector of the atomic electron ( $r_{\text{rms}} \sim n^2/Z_1$ , where  $Z_1$  is the nuclear charge), and  $R$  is the separation between the nucleus of the radiating atom/ion and the nearest perturbing ion. We use the atomic units here and below.

The dipole term of the expansion ( $\sim 1/R^2$  or  $\sim F$ ) does not lead to any shift of a hydrogenic SL. Indeed, each pair of the Stark components, characterized by the electric quantum numbers  $q$  and  $-q$ , is symmetric with respect to the unperturbed frequency  $\omega_0$  of the hydrogenic line – symmetric concerning both the displacement from  $\omega_0$  and the intensity. Here  $q = n_1 - n_2$ , where  $n_1$  and  $n_2$  are the first two of the three parabolic quantum numbers ( $n_1 n_2 m$ ). The next, quadrupole term of the expansion ( $\sim 1/R^3$  or  $\sim F^{3/2}$ ) does not shift the center of gravity of hydrogenic lines. This was proven analytically in paper [12]. Namely, after allowing for the quadrupole corrections to both the energies/frequencies and the intensities, and then summing up over all Stark components of a hydrogenic SL, the center of gravity shift becomes exactly zero at any fixed value of  $R$  or  $F$ .

Thus, within the approach based on the multipole expansion, the first non-vanishing ionic contribution to the shift of hydrogenic SL is supposed to originate from the next term of the multipole expansion: from the term  $\sim 1/R^4$  or  $\sim F^2$ . In processing this term, many authors considered only the quadratic Stark (QS) effect – see papers [8, 13, 14]:

$$\Delta E_{QS}^{(4)} = -\frac{Z_2^2 n^4}{16 Z_1^4 R^4} (17n^2 - 3q^2 - 9m^2 + 19) \quad (1)$$

Here  $Z_2$  is the charge of perturbing ions; the superscript (4) at  $\Delta E_{QS}$  specifies that this term is of the 4<sup>th</sup> order with respect to the small parameter  $r_{\text{rms}}/R$ .

However, first, the corrections of this order to the energies are of the same order as the corrections to the intensities, as noted in paper [15]. Therefore, calculations in papers [13, 14] were inconsistent because they took into account the quadratic Stark corrections only to energies. Second, there is an even more important flaw in papers [8, 13, 14], as follows.

The above Eq. (1) was obtained using the dipole term of the multipole expansion treated in the 2<sup>nd</sup> order of the perturbation theory. However, the quadrupole term, processed in the 2<sup>nd</sup> order of the perturbation theory, and the octupole term, processed in the 1<sup>st</sup> order of the perturbation theory, in fact also yield energy corrections  $\sim 1/R^4$  – this was shown as early as in 1969 by Sholin [16]. The rigorous energy correction of the order  $\sim 1/R^4$  can be obtained in the form (given in paper [16] and presented also in book [17]):

$$\Delta E^{(4)} = \frac{Z_2 n^3}{16 Z_1^4 R^4} \left[ Z_1 q (109q^2 - 39n^2 - 9m^2 + 59) - Z_2 n (17n^2 - 3q^2 - 9m^2 + 19) \right]. \quad (2)$$

Apparently, it is inconsistent to allow for one term and to neglect two other terms of the same order of magnitude.

Nevertheless, from table III of paper [8] it is clear that the ionic shift  $\Delta E^{(4)}$  due to the quadratic Stark effect is by one or more orders of magnitude smaller than the corresponding electronic shift (and that while the latter is red, the former is blue). A more consistent calculation of the ionic shift  $\Delta E^{(4)}$  does not change the fact that it is just a very small correction to the corresponding electronic shift and is even a smaller correction to the sum of the corresponding electronic shift and the PPS. Therefore, the standard shift can be represented with the accuracy, sufficient for comparison with experiments, by the sum of the electronic shift and the PPS, while the standard ionic shift can be neglected.

### 3. NEW SOURCE OF SHIFT: ANALYTICAL CALCULATIONS AND COMPARISON WITH EXPERIMENT

The standard approaches to calculating the ionic shift disregarded configurations where  $r_{\text{rms}}/R > 1$ , *i.e.*, where the nearest perturbing ion is within the radiating atom/ion (below we call them “penetrating configurations”). In the standard approaches, all terms of the multipole expansion, starting from the quadrupole term, at the averaging over the distribution of the quantity  $R$ , resulted in integrals diverging at small  $R$ , which were evaluated one way or another, *e.g.*, by introducing cutoffs. However, the fact of the divergence of these integrals should have been a warning that the standard approach did not provide a consistent complete description of the ionic shift.

The contribution to the ionic shift from penetrating configurations is a product of two factors. The first fact is the statistical weight of penetrating configurations, which is relatively small. The second factor is the shift relevant to penetrating configurations is relatively large. We show below that the product of these two factors can exceed the total standard shift represented by the sum of the electronic shift and the PPS.

For penetrating configurations, we use the expansion in terms of the parameter  $R/r_{\text{rms}} < 1$  in the basis of the spherical wave functions of the so-called “united atom”, the latter being a hydrogenic ion of the nuclear charge  $Z_1 + Z_2$ . The expansion of the energy can be represented in the form (see, *e.g.*, Eqs. (5.10 – 5.12) from book [17]):

$$E = -\frac{(Z_1 + Z_2)^2}{2n^2} + \mathcal{O}\left(\frac{R^2}{r_{\text{rms}}^2}\right). \quad (3)$$

Thus, the first non-vanishing contribution  $S(n)$  to the shift of the energy level is indeed relatively large:

$$S(n) = -\frac{(Z_1 + Z_2)^2}{2n^2} - \frac{Z_1^2}{2n^2} = -\frac{2Z_1Z_2 + Z_2^2}{2n^2}. \quad (4)$$

Below in order to simplify formulas, while still getting the message across, we limit ourselves by the practically important case where  $Z_1 = Z_2 = Z$ . According to Eqs. (5.11), (5.12) from book [17] (but noting there the error in the sign of Eq. (5.11)), the perturbed energies  $E_{nlm}$  for  $l > 0$  are given by:

$$E_{nlm} = -\frac{Z^2}{2n^2} - \frac{8[1(1+1) - 3m^2]}{nl(l+1)(2l-1)(2l+1)(2l+3)} Z^4 R^2. \quad (5)$$

For the case of  $l = 0$ , the relation simplifies to:

$$E_{n00} = -\frac{Z^2}{2n^2} + \frac{8Z^4 R^2}{3n^3}. \quad (6)$$

For the specific perturbed eigenvalues of the  $n = 1$ ,  $n = 2$ , and  $n = 3$  levels, respectively, we obtain the following correction terms (*i.e.*, below are only the terms  $\sim R^2$ ):

$$\begin{aligned} E_{100} &= \frac{8}{3} Z^4 R^2, \quad E_{200} = \frac{1}{3} Z^4 R^2, \quad E_{210} = -\frac{1}{15} Z^4 R^2, \quad E_{21\pm 1} = \frac{1}{30} Z^4 R^2, \quad E_{300} = \frac{8}{81} Z^4 R^2, \quad E_{310} = -\frac{8}{405} Z^4 R^2, \\ E_{31\pm 1} &= \frac{4}{405} Z^4 R^2, \quad E_{320} = -\frac{8}{2835} Z^4 R^2, \quad E_{32\pm 1} = -\frac{4}{2835} Z^4 R^2, \quad E_{32\pm 1} = \frac{8}{2835} Z^4 R^2. \end{aligned} \quad (7)$$

The unperturbed energies are the eigenvalues corresponding to the united atom of the nuclear charge  $2Z$ . Then the perturbed energies (counted from the united atom unperturbed energies) acquire an additional correction with respect to the unperturbed energies. The perturbed energies are then:

$$\begin{aligned}
 E_{100} &= -\frac{3}{2}Z^2 + \frac{8}{3}Z^4R^2, & E_{200} &= -\frac{3}{8}Z^2 + \frac{1}{3}Z^4R^2, & E_{210} &= -\frac{3}{8}Z^2 - \frac{1}{15}Z^4R^2, & E_{21\pm 1} &= -\frac{3}{8}Z^2 + \frac{1}{30}Z^4R^2, \\
 E_{300} &= -\frac{1}{6}Z^2 + \frac{8}{81}Z^4R^2, & E_{310} &= -\frac{1}{6}Z^2 - \frac{8}{405}Z^4R^2, & E_{31\pm 1} &= -\frac{1}{6}Z^2 + \frac{4}{405}Z^4R^2, & E_{320} &= -\frac{1}{6}Z^2 - \frac{8}{2835}Z^4R^2, \\
 E_{32\pm 1} &= -\frac{1}{6}Z^2 - \frac{4}{2835}Z^4R^2, & E_{32\pm 1} &= -\frac{1}{6}Z^2 + \frac{8}{2835}Z^4R^2.
 \end{aligned}
 \tag{8}$$

**Lyman- $\alpha$  Line**

For any hydrogenic spectral line, the total intensity of  $\sigma$ -components is twice the intensity of all  $\pi$ -components. In particular, the Lyman- $\alpha$  line, the total intensity of the  $\sigma$ -components, which consists of the 21-1 and 211 sublevel, is twice the intensity of the single  $\pi$ -component, which consists of the 210 sublevel.

The total normalized shift of the Lyman- $\alpha$  line is given by:

$$S(R) = \frac{\sum_k I_k (E_k(n=2) - E_k(n=1))}{\sum_k I_k},
 \tag{9}$$

where  $k$  represents the  $k^{\text{th}}$  component to the total shift of the spectral line. The obtained result is:

$$S(R) = \frac{1}{3} \left( -\frac{3}{8}Z^2 - \frac{1}{15}Z^4R^2 \right) + \frac{1}{3} \left( -\frac{3}{8}Z^2 + \frac{1}{3}Z^4R^2 \right) + \frac{2}{3} \left( -\frac{3}{8}Z^2 + \frac{1}{30}Z^4R^2 \right) - \left( -\frac{3}{2}Z^2 + \frac{8}{3}Z^4R^2 \right)
 \tag{10}$$

which is left unsimplified here.

The next step is to average this shift over the appropriate distribution  $P_u(u) = P_u(R/R_0)$  of the internuclear distances, scaled by the mean interionic distance

$$R_0 = \left( \frac{3Z}{4\pi N_e} \right)^{\frac{1}{3}},
 \tag{11}$$

where  $N_e$  is the electron density. Since we consider here penetrating configurations, where the nearest neighbor ion is inside the electron cloud, then the distribution  $P_u(R/R_0)$  can be obtained from the binary distribution  $P_w(w) = P_w(F/F_0)$  of the ion microfield (where  $F = Z_2/R^2$  and  $F_0 = Z_2/R_0^2$ , so that  $u = 1/w$ ) presented in papers [18, 19], as follows. Since

$$P_u(u) du = -P_w(w) dw,
 \tag{12}$$

then for  $P_u(u)$  we get

$$P_u(u) = \left( \frac{2}{u^3} \right) P_w \left( \frac{1}{u^2} \right).
 \tag{13}$$

Using the results from papers [18, 19], for the case of  $Z_1 = Z_2 \equiv Z$ , the ion microfield distribution can be normalized analytically and brought to the form

$$P_w(w) = \frac{\left( \frac{3^{\frac{1}{2}} \pi}{w^{\frac{5}{2}}} \right) \exp \left( -\frac{1}{\frac{3}{w^2}} - kw^2 \right)}{\text{MeijerG} \left[ \left\{ \left\{ \right\}, \left\{ \right\} \right\}, \left\{ \left\{ 0, \frac{1}{3}, \frac{2}{3}, 1 \right\}, \left\{ \right\} \right\}, \frac{k^3}{27} \right]}.
 \tag{14}$$

where Meijer  $G[\cdot]$  is the Meijer  $G$ -function and

$$k = \frac{T_e Z^2 v^2}{2qT_i}, \quad q = \frac{15}{4(2\pi)^{\frac{1}{2}}} = 1.496, \quad v = \frac{R_0}{r_{De}}, \quad r_{De} = \left( \frac{T_e}{4\pi e^2 N_e} \right)^{\frac{1}{2}}, \quad (15)$$

the latter being the Debye radius. A practical formula for the quantity  $v$  is

$$v = 8.98 \times 10^{-2} \left[ N_e (cm^{-3}) \right]^{\frac{1}{6}} / \left[ T_e (K) \right]^{\frac{1}{2}}. \quad (16)$$

In Eqs. (15) and (16),  $T_e$  and  $T_i$  are the electron and ion temperatures, respectively.

Then according to Eq. (13), for the distribution  $P_u(u)$  we get

$$P_u(u) = \frac{2\pi^{\frac{1}{2}} u^2 \exp\left(-u^3 - \frac{k}{u}\right)}{\text{Meijer } G\left[\left\{\left\{\right\}, \left\{\right\}\right\}, \left\{\left\{0, \frac{1}{3}, \frac{2}{3}, 1\right\}, \left\{\right\}\right\}, \frac{k^3}{27}\right]}. \quad (17)$$

The averages of various powers of  $u = R/R_0$  can be also expressed via various Meijer  $G$ -functions as follows:

$$\int_0^{\infty} u^4 P_u(u) du = \frac{k^{10} \text{Meijer } G\left[\left\{\left\{\right\}, \left\{\right\}\right\}, \left\{\left\{-\left(\frac{5}{3}\right), -\left(\frac{3}{2}\right), -\left(\frac{4}{3}\right), -\left(\frac{7}{6}\right), -1, -\left(\frac{5}{6}\right), 0\right\}, \left\{\right\}\right\}, \frac{k^6}{46656}\right]}{80621568\sqrt{3}\pi^{\frac{5}{2}}C}, \quad (18)$$

$$\int_0^{\infty} u^5 P_u(u) du = \frac{k^{12} \text{Meijer } G\left[\left\{\left\{\right\}, \left\{\right\}\right\}, \left\{\left\{-2, -\left(\frac{11}{6}\right), -\left(\frac{5}{3}\right), -\left(\frac{3}{2}\right), -\left(\frac{4}{3}\right), -\left(\frac{7}{6}\right), 0\right\}, \left\{\right\}\right\}, \frac{k^6}{46656}\right]}{8707129344\sqrt{3}\pi^{\frac{5}{2}}C}, \quad (19)$$

$$\int_0^{\infty} u^6 P_u(u) du = \frac{k^{14} \text{Meijer } G\left[\left\{\left\{\right\}, \left\{\right\}\right\}, \left\{\left\{-\left(\frac{7}{3}\right), -\left(\frac{13}{6}\right), -2, -\left(\frac{11}{6}\right), -\left(\frac{5}{3}\right), -\left(\frac{3}{2}\right), 0\right\}, \left\{\right\}\right\}, \frac{k^6}{46656}\right]}{313456656384\sqrt{3}\pi^{\frac{5}{2}}C} \quad (20)$$

where

$$C = \frac{\sqrt{3}}{4\pi^{\frac{5}{2}}} \text{Meijer } G\left[\left\{\left\{\right\}, \left\{\right\}\right\}, \left\{\left\{0, \frac{1}{6}, \frac{1}{3}, \frac{1}{2}, \frac{2}{3}, \frac{5}{6}, 1\right\}, \left\{\right\}\right\}, \frac{k^6}{46656}\right], \quad (21)$$

However, from these general results it would be difficult to study asymptotics because Taylor expansions of MeijerG-functions are not available. More explicit results are possible to obtain for relatively low-density plasmas, where the distribution from Eq. (11) reduces to:

$$P(R) = 3 \frac{R^2}{R_0^3} \exp\left(-\frac{R^3}{R_0^3}\right). \quad (22)$$

(here we assumed again  $Z_1 = Z_2 = Z$ ).

Let us consider the limits of integration. We can approximate the upper limit of integration as the root mean square matrix element of the radial integral, which depends on the sublevel in consideration. This relation is:

$$r_{\text{rms}} = \sqrt{\frac{3n^2}{4Z^2} [(5n^2 + 1 - 3l(l+1))]} \quad (23)$$

After averaging over  $l$ , we obtain:

$$r_n = \left[ \frac{3n^2(7n^2 + 5)}{8Z^2} \right]^{\frac{1}{2}} \quad (24)$$

(here and below we omit the subscript “rms”).

From Eq. (24), we find the upper limits of integration for the  $n = 1$  and  $n = 2$  levels, respectively, to be:

$$r_1 = \left(\frac{9}{2}\right)^{\frac{1}{2}} \frac{1}{Z}, \quad r_2 = \left(\frac{11}{2}\right)^{\frac{1}{2}} \frac{3}{Z}. \quad (25)$$

Therefore, we can calculate the averaged shift due to penetrating ions (keeping terms up to  $\sim R^5$ ) as follows:

$$S_{\text{ave}} = \int_0^{r_2} \left\{ \frac{1}{3} \left( -\frac{3}{8} Z^2 - \frac{1}{15} Z^4 R^2 \right) + \frac{1}{3} \left( -\frac{3}{8} Z^2 + \frac{1}{3} Z^4 R^2 \right) + \frac{2}{3} \left( -\frac{3}{8} Z^2 + \frac{1}{30} Z^4 R^2 \right) \right\} 3 \frac{R^2}{R_0^3} \exp\left(-\frac{R^3}{R_0^3}\right) dR - \int_0^{r_1} \left( -\frac{3}{2} Z^2 + \frac{8}{3} Z^4 R^2 \right) 3 \frac{R^2}{R_0^3} \exp\left(-\frac{R^3}{R_0^3}\right) dR, \quad (26)$$

where upon expansion of the distribution,  $S_{\text{ave}}$  is:

$$S_{\text{ave}} = \int_0^{\left(\frac{11}{2}\right)^{\frac{1}{2}} \frac{3}{Z}} \left\{ -\frac{9Z^2 R^2}{8R_0^3} + \frac{9Z^2 R^5}{8R_0^6} + \dots \right\} dR - \int_0^{\left(\frac{9}{2}\right)^{\frac{1}{2}} \frac{1}{Z}} \left\{ -\frac{9Z^2 R^2}{2R_0^3} + \frac{8Z^4 R^4}{R_0^6} + \frac{9Z^2 R^5}{2R_0^6} + \dots \right\} dR \approx -\frac{88.2}{ZR_0^3}. \quad (27)$$

Then we substitute  $R_0$  from Eq. (11), so that Eq. (27) reduces to the following:

$$S_{\text{ave}} = -\frac{370Ne}{Z^2}.$$

### Lyman-β Line

Similarly to the above calculations for the Lyman-α line, by using the relative intensities of the line components and the perturbation to the energies, we obtain the following expression for the shift of the Lyman-β line:

$$S(R) = \frac{1}{3} \left[ \left( -\frac{Z^2}{6} + \frac{8Z^4 R^2}{81} \right) + \left( -\frac{Z^2}{6} - \frac{8Z^4 R^2}{405} \right) + \left( -\frac{Z^2}{6} - \frac{8Z^4 R^2}{2835} \right) \right] + \frac{2}{3} \left[ \left( -\frac{Z^2}{6} + \frac{4Z^4 R^2}{405} \right) + \left( -\frac{Z^2}{6} - \frac{4Z^4 R^2}{2835} \right) \right] - \left( \frac{3Z^2}{2} + \frac{8}{3} Z^4 R^2 \right). \quad (29)$$

Just as for the Lyman- $\alpha$  line, we average this shift over the same distribution  $P(R)$  from Eq. (16) and use the same upper limit of integration for the  $n = 1$  level. For the  $n = 3$  level, according to Eq. (24), the upper limit of integration is:

$$r_3 = \left(\frac{51}{2}\right)^{\frac{1}{2}} \frac{3}{Z}. \quad (30)$$

Then the averaged shift of the Lyman- $\beta$  line due to penetrating ions (keeping terms up to  $\sim R^5$ ) is given by:

$$S_{\text{ave}} = \int_0^{r_3} \left\{ \frac{1}{3} \left[ \left( -\frac{Z^2}{6} + \frac{8Z^4 R^2}{81} \right) + \left( -\frac{Z^2}{6} - \frac{8Z^4 R^2}{405} \right) + \left( -\frac{Z^2}{6} - \frac{8Z^4 R^2}{2835} \right) \right] + \frac{2}{3} \left[ \left( -\frac{Z^2}{6} + \frac{4Z^4 R^2}{405} \right) + \left( -\frac{Z^2}{6} - \frac{4Z^4 R^2}{2835} \right) \right] \right\} \frac{3R^2}{R_0^3} \exp\left(-\frac{R^3}{R_0^3}\right) dR - \int_0^{r_3} \left( -\frac{3}{2} Z^2 + \frac{8}{3} Z^4 R^2 \right) 3 \frac{R^2}{R_0^3} \exp\left(-\frac{R^3}{R_0^3}\right) dR, \quad (31)$$

where upon expansion of the distribution,  $S_{\text{ave}}$  is:

$$S_{\text{ave}} = \int_0^{\left(\frac{51}{2}\right)^{\frac{1}{2}} \frac{3}{Z}} \left\{ -\frac{Z^2 R^2}{2R_0^3} + \frac{Z^2 R^5}{2R_0^6} + \dots \right\} dR - \int_0^{\left(\frac{9}{2}\right)^{\frac{1}{2}} \frac{1}{Z}} \left\{ -\frac{9Z^2 R^2}{2R_0^3} + \frac{8Z^4 R^4}{R_0^3} + \frac{9Z^2 R^5}{2R_0^6} + \dots \right\} dR \approx -\frac{333}{ZR_0^3}. \quad (32)$$

Then we substitute  $R_0$  from Eq. (11), so that Eq. (33) reduces to the following:

$$S_{\text{ave}} = -\frac{1.39 \times 10^3 Ne}{Z^2}. \quad (33)$$

### Balmer- $\alpha$ Line

The calculation for the Balmer- line is similar to the above calculations for the Lyman-alpha and Lyman-beta lines, though it is more involved. It yields

$$S(R) = \left( -\frac{Z^2}{6} + \frac{40Z^4 R^2}{25461} + \frac{128Z^6 R^4}{89667} \right)_3 - \left( -\frac{3Z^2}{8} + \frac{160Z^4 R^2}{2829} + \frac{101Z^6 R^4}{9430} \right)_2, \quad (34)$$

where the subscripts refer to the levels  $n = 3$  and  $n = 2$ , respectively. It is important to separate the results between levels for averaging over  $R$  since the limits of integration differ between the levels. Then the averaged shift of the Balmer- line due to penetrating ions is given by:

$$S_{\text{ave}} = \int_0^{r_3} \left( -\frac{Z^2}{6} + \frac{40Z^4 R^2}{25461} + \frac{128Z^6 R^4}{89667} \right) \frac{3R^2}{R_0^3} \exp\left(-\frac{R^3}{R_0^3}\right) dR - \int_0^{r_2} \left( -\frac{3Z^2}{8} + \frac{160Z^4 R^2}{2829} + \frac{101Z^6 R^4}{9430} \right) \frac{3R^2}{R_0^3} \exp\left(-\frac{R^3}{R_0^3}\right) dR, \quad (35)$$

where upon expansion of the distribution,  $S_{\text{ave}}$  is

$$S_{\text{ave}} = \int_0^{\left(\frac{51}{2}\right)^{\frac{1}{2}} \frac{3}{Z}} \left\{ -\frac{Z^2 R^2}{2R_0^3} + \frac{40Z^4 R^4}{8487R_0^3} + \frac{Z^2 R^5}{2R_0^6} + \dots \right\} dR - \int_0^{\left(\frac{11}{2}\right)^{\frac{1}{2}} \frac{3}{Z}} \left\{ -\frac{9Z^2 R^2}{8R_0^3} + \frac{160Z^4 R^4}{943R_0^3} + \frac{9Z^2 R^5}{8R_0^6} + \dots \right\} dR \approx -\frac{184}{ZR_0^3}. \quad (36)$$

Then we substitute  $R_0$  from Eq. (11), so that Eq. (33) reduces to the following:

$$S_{\text{ave}} = -\frac{769N_e}{Z^2}. \tag{37}$$

As an example, we compare various theoretical sources of the shift (including our result) for the He II Balmer- $\alpha$  line with the experimental shift of this line obtained by Pittman and Fleurier [5] for the electron densities in the range of  $N_e = (0.3 - 2.3) \times 10^{17} \text{ cm}^{-3}$ . In Figure 1, the experimental shifts  $\Delta\lambda_{\text{exp}}$  are shown by circles. The theoretical shift by Griem [6, 8]  $\Delta\lambda_{\text{Griem}}$ , with which Pittman and Fleurier [5] compared their experimental results, is shown by the dashed blue line.

It is seen that there was a huge discrepancy between the experimental red shift  $\Delta\lambda_{\text{exp}}$  and the theoretical red shift by Griem

$$\Delta\lambda_{\text{Griem}} \text{ (mÅ)} = 9.4N_e \text{ (cm}^{-3}\text{)}/10^{17}. \tag{38}$$

The discrepancy is by a factor of 2.6 at  $N_e = 10^{17} \text{ cm}^{-3}$  and increasing to almost a factor of five at  $N_e = 2.2 \times 10^{17} \text{ cm}^{-3}$ .

Griem’s shift [6, 8] is a well-established part of the “standard shifts”. The other part – plasma polarization shift (PPS) – has a factor of two difference in calculations by different authors. For example, from the results of the paper Benredjem *et. al.* [20], the PPS of the three components of the He II Balmer-alpha line at  $T = 4 \text{ eV}$  can be deduced to be as follows.

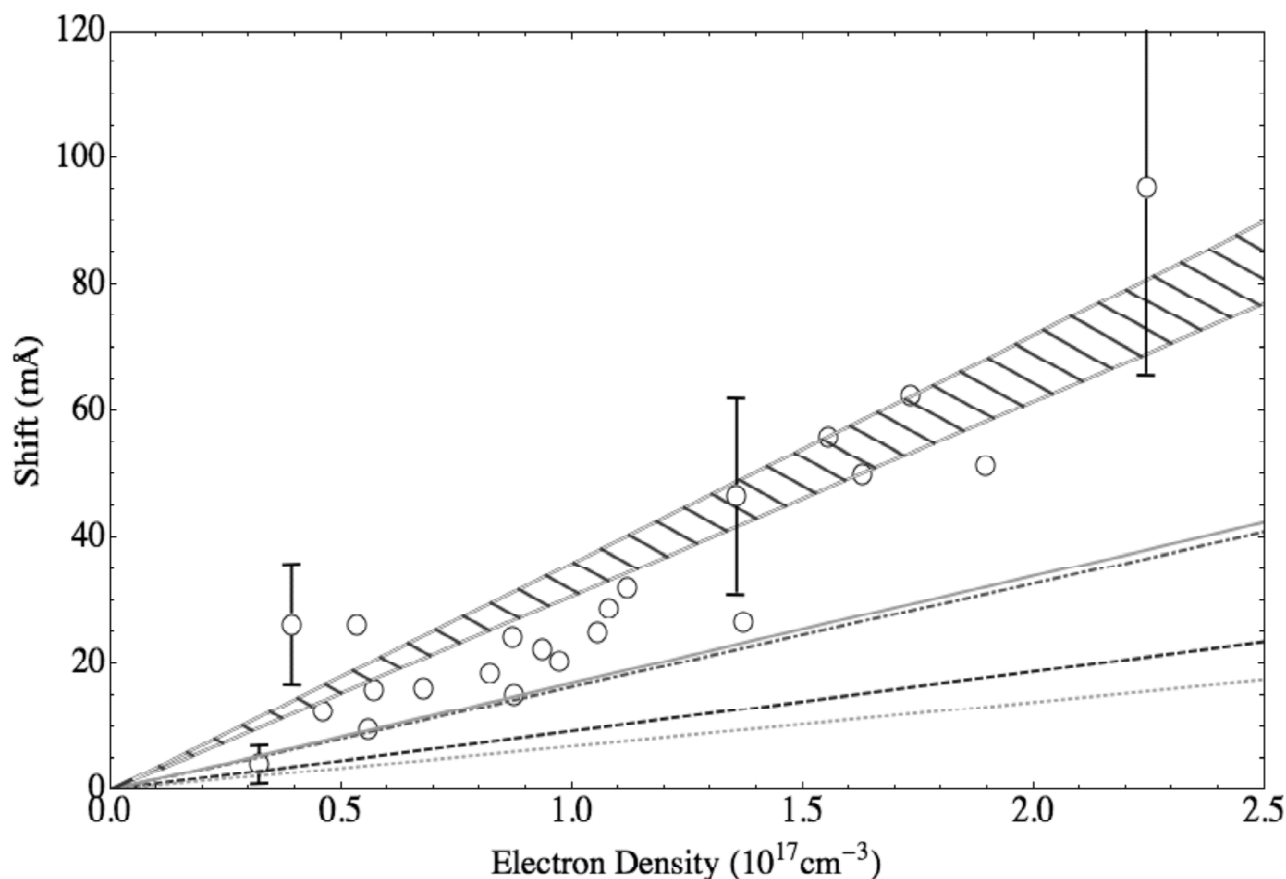


Figure 1: Comparison of the experimental shift of the He II Balmer-alpha line 1640 Å measured by Pittman and Fleurier [5], shown by circles, with the following theoretical shifts: Griem’s shift [6, 8] – dashed blue line; plasma polarization shift – dotted orange line; the sum of the latter two theoretical shifts – dashed-dotted red line; shift due to penetrating ions (introduced in the present paper) – solid green line; the sum of all three theoretical shifts – purple band, the width of which reflects the theoretical error. The experimental error bars are shown only for few electron densities in order to avoid making the figure too “busy” and difficult to understand.

For  $3d-2p$ :  $\Delta\lambda_{\text{PPS}}(\text{mÅ}) = 8.5N_e(\text{cm}^{-3})/10^{17}$ . (Relative intensity 0.814422)

For  $3p-2s$ :  $\Delta\lambda_{\text{PPS}}(\text{mÅ}) = 11.8N_e(\text{cm}^{-3})/10^{17}$ . (Relative intensity 0.169671)

For  $3s-2p$ :  $\Delta\lambda_{\text{PPS}}(\text{mÅ}) = 14.8N_e(\text{cm}^{-3})/10^{17}$ . (Relative intensity 0.0159067)

The average is:  $\Delta\lambda_{\text{PPS}}(\text{mÅ}) = 9.2N_e(\text{cm}^{-3})/10^{17}$ .

On the other hand, there are PPS calculations by Blaha and Davis [21] for He II 1640 Å, quoted by Marangos *et al.* [22]. For Blaha-Davis' case B, which is the more realistic than case A, at  $N_e = 2 \times 10^{18} \text{ cm}^{-3}$  and  $T = 3.3 \text{ eV}$ , it yielded  $\Delta\lambda_{\text{PPS}} = 100 \text{ mÅ}$ , thus corresponding to  $\Delta\lambda_{\text{PPS}}(\text{mÅ}) = 5 N_e(\text{cm}^{-3})/10^{17}$ .

At the temperature  $T = 4 \text{ eV}$ , relevant to Pittman-Fleurier experiment [5], the PPS would be slightly less than  $5N_e(\text{cm}^{-3})/10^{17}$  because it decreases as the temperature increases.

So, for the comparison with Pittman-Fleurier experiment [5] we adopt the theoretical PPS averaged over the above two sets of theoretical calculations, namely:

$$\Delta\lambda_{\text{PPS}}(\text{mÅ}) = 7N_e(\text{cm}^{-3})/10^{17}. \quad (39)$$

In Figure 1 it is shown by the dotted orange line.

The sum  $\Delta\lambda_{\text{Griem}} + \Delta\lambda_{\text{PPS}}$  is shown by the dash dotted red line. It is seen that even after adding the PPS to Griem's shift, their sum still underestimates the experimental shift at least by a factor of two.

As for the new source of shift presented in our paper – the shift due to penetrating ions  $\Delta\lambda_{\text{PI}}$  – for the He II Balmer- $\alpha$  line it is given by:

$$\Delta\lambda_{\text{PI}}(\text{mÅ}) = 17N_e(\text{cm}^{-3})/10^{17}. \quad (40)$$

In Figure 1 it is shown by the solid green line. The sum  $\Delta\lambda_{\text{Griem}} + \Delta\lambda_{\text{PPS}} + \Delta\lambda_{\text{PI}}$  is presented in Figure 1 by the dashed purple band. (The width of the band reflects the theoretical error of this sum.) It is seen that adding the shift due to the penetrating ions brings the total shift into a good agreement with the experimental shift.

### 3. CONCLUSIONS

We introduced an additional source of the shift of H-like spectral lines arising from the configurations where the nearest perturbing ion is within the radiating atom/ion ("penetrating configurations"). We demonstrated, as an example, that for the He II Balmer-alpha line it makes the primary contribution to the total red shift and brings the total theoretical shift in a good agreement with the experimental shift measured by Pittman and Fleurier [5], while without the allowance for penetrating configurations the discrepancy between theoretical and experimental shifts was by factors between two and five.

It is important to emphasize that our relatively simple model does not apply to some radiator-perturber combinations. Let us consider, *e.g.*, hydrogen or deuterium spectral lines. At low principal quantum numbers, such as, *e.g.*,  $n = 1 - 3$ , the penetrating configuration – a proton inside the hydrogen or deuterium atom – corresponds to the proton-proton or proton-deuteron separation of the same order of magnitude as in the molecules  $\text{H}_2^+$  or  $\text{HD}^+$  (if hydrogen/deuterium lines are emitted from hydrogen/deuterium plasmas), or in the molecules  $\text{HeH}^{2+}$  and  $\text{HeD}^{2+}$  (if hydrogen/deuterium lines are emitted from helium plasmas). Therefore, in this case the presence of the bonding molecular orbital has to be taken into account, which is beyond our relatively simple model.

However, for the spectral lines of hydrogenic helium (He II) emitted from helium plasmas, our simple model applies because the corresponding would-be molecule  $\text{He}_2$  and its ions, such as, *e.g.*,  $\text{He}_2^{3+}$ , do not exist. Similarly, for the lines of hydrogenic beryllium (Be IV) emitted from beryllium plasmas, our simple model applies because the corresponding would-be molecule  $\text{Be}_2$  and its ions, such as, *e.g.*,  $\text{Be}_2^{7+}$ , do not exist. In fact, our relatively simple model applies to most pairs consisting of a heavy hydrogenic ion and a heavy perturbing, fully-stripped ion – because for the overwhelming majority of such combinations the bonding molecular orbitals do not exist.

---

**REFERENCES**

- [1] H. Nussbaumer and L. Bieri, *Discovering the Expanding Universe* (Cambridge Univ. Press, Cambridge) 2009.
- [2] H.R. Griem, *Principles of Plasma Spectroscopy* (Cambridge Univ. Press, Cambridge) 1997, Sect. 4.10.
- [3] E. Oks, *Stark Broadening of Hydrogen and Hydrogenlike Spectral Lines in Plasmas: The Physical Insight* (Alpha Science International, Oxford) 2006, Sects. 2.6, 6.
- [4] C.G. Parigger, D.H. Plemmons, and E. Oks, *Applied Optics* **42** (2003) 5992.
- [5] T.L. Pittman and C. Fleurier, *Phys. Rev. A* **33** (1986) 1291.
- [6] H.R. Griem, *Phys. Rev. A* **28** (1983) 1596.
- [7] D.B. Boercker and C.A. Iglesias, *Phys. Rev. A* **30** (1984) 2771.
- [8] H.R. Griem, *Phys. Rev. A* **38** (1988) 2943.
- [9] D. Salzman, *Atomic Physics in Hot Plasmas* (Oxford Univ. Press, Oxford) 1998.
- [10] O. Renner *et. al.*, *J. Phys. B: At. Mol. Opt. Phys.* **31** (1998) 1379.
- [11] H.F. Berg, A.W. Ali, R. Lincke, and H.R. Griem, *Phys. Rev.* **125** (1962) 199.
- [12] E. Oks, *J. Quant. Spectrosc. Rad. Transfer* **58** (1997) 821.
- [13] A. Könies and S. Günter, *J. Quant. Spectrosc. Rad. Transfer* **52** (1994) 825.
- [14] S. Günter and A. Könies, *Phys. Rev. E* **55** (1977) 907.
- [15] A.V. Demura, V. Helbig, and D. Nikolic, in *Spectral Line Shapes, 16<sup>th</sup> ICSSL*, edit. C.A. Back, AIP Conf. Proc. **645** (2002) 318.
- [16] G.V. Sholin, *Opt. Spectrosc.* **26** (1969) 275.
- [17] I.V. Komarov, L.I. Ponomarev, and S. Yu. Slavyanov, *Spheroidal and Coulomb Spheroidal Functions* (Nauka, Moscow) 1976, in Russian.
- [18] B. Held, *J. Physique* **45** (1984) 1731.
- [19] B. Held, C. Deutsch, and M.-M. Gombert, *Phys. Rev. A* **29** (1984) 880.
- [20] D.E. Benredjem, Hoe Nguen, and G. Couland, *J. Quant. Spectrosc. Rad. Transfer* **43** (1990) 415.
- [21] M. Blaha and J. Davis, *NRL Memorandum Report* 5155 (1983).
- [22] J.P. Marangos, D.D. Burgess, and K.G.H. Baldwin, *J. Phys. B: At. Mol. Opt. Phys.* **21** (1988) 3357.